CHARACTERIZATION OF REGENERATED CELLULOSE FILMS FROM OIL PALM EMPTY FRUIT BUNCH INCORPORATED WITH $BiFeO_3$ AS A POTENTIAL PHOTOCATALYST

POONANULKARAGE RUWAN DINESH WEERASOORIYA

UNIVERSITI SAINS MALAYSIA

2022

CHARACTERIZATION OF REGENERATED CELLULOSE FILMS FROM OIL PALM EMPTY FRUIT BUNCH INCORPORATED WITH $BiFeO_3$ AS A POTENTIAL PHOTOCATALYST

by

POONANULKARAGE RUWAN DINESH WEERASOORIYA

Thesis submitted in fulfilment of the requirements
for the degree of
Doctor of Philosophy

April 2022

ACKNOWLEDGEMENT

This doctoral thesis only became a reality with the guidance and immense support of several individuals. I would like to express my sincere gratitude to all those individuals who were with me throughout this endeavor.

First and foremost, let me appreciate the knowledge sharing, guidance, support and the company of my main supervisor, Associate Professor Dr. Mohamad Haafiz Mohamad Kassim. I would extend my sincere gratitude for all that he has been in making my thesis a success. Also, let me extend my gratitude to my co-supervisors, Professor TS. Datuk Dr. Abdul Khalil Bin HP Shawkataly and Associate Professor Dr. Noor Haida Binti Mohd Kaus, for the guidance and valuable inputs without which my thesis would not follow a smooth journey.

A very special note of thanks goes to the financial assistance provided for each and every laboratory experiment through Fundamental Research Grant Scheme FRGS/1/2019/STG07/USM/02/15 by the Ministry of Higher Education, Malaysia, and the Research University Grant Scheme (RU) 1001/PTEKIND/8011108 by Universiti Sains Malaysia.

I would extend my sincere gratitude to all laboratory staff of School of Industrial Technology, for their assistance and continuous support during the laboratory experiments. Also, my gratitude goes to laboratory staff of School of Archeology, Science and Engineering Research Centre (SERC) and Institute for Research in Molecular Medicine (INFORMM) for their truthful commitments in making my laboratory experiments a success. My sincere gratitude goes towards Dr. Md Sohrab Hossain for his guidance and support for the publications. Let me also

thank my BRTech postgraduate room colleagues for their continuous support and companionship during my hardships.

Lastly, my heartfelt gratitude goes my family for the continuous love and strength they have given me during the PhD career. Special note of appreciation and love goes to my loving wife and little daughter for letting me pursue my dreams and tolerating my absence. I would like to thank my father who has left this world, for his love and caring towards me since my childhood. Then I have no words to appreciate my mother for her continuous follow up about me. I thank my mother for being with me always to share my genuine feelings. Also, I thank my elder sister who was my family teacher until I become a teenager. She was my first role model and the greatest motivation behind my academic journey this long. Also, I thank to my extended family for all their support and love. Finally, I don't forget to thank all of my best friends who are in my inner circle.

TABLE OF CONTENTS

ACKNOWLEDGEMENT ..... **ii**

TABLE OF CONTENTS ..... **iv**

LIST OF TABLES ..... **viii**

LIST OF FIGURES ..... **x**

LIST OF SYMBOLS ..... **xiv**

LIST OF ABBREVIATIONS ..... **xv**

LIST OF APPENDICES ..... **xviii**

ABSTRAK ..... **xix**

ABSTRACT ..... **xxi**

CHAPTER 1 INTRODUCTION **1**

1.1 General Introduction 1

1.2 Background 2

1.3 Problem Statement 3

1.4 Scope of the study 4

1.5 Gap of novelty 5

1.6 Objectives 6

CHAPTER 2 LITERATURE REVIEW **7**

2.1 General Overview 7

2.1 Biopolymers 8

2.2 Development of cellulose dissolution processes 11

2.2.1 Cellulose and its nature 11

2.2.2 Cellulose Dissolution 13

2.2.2(a) Preliminary research works 13

2.2.2(b) Ionic liquids 17

2.2.2(c) [BMIM]Cl 19

2.2.2(d) Advantages of ionic liquids 20

2.2.2(e) Dissolution process of cellulose 21

2.3 Regenerated cellulose 23

2.4 Microcrystalline cellulose (MCC) and experimental selection for optimizing the process 24

2.5 Photocatalytic degradation 26

2.6 Bismuth ferrite 27

2.7 Factors affecting on effective photocatalytic degradation 29

2.8 Selection of experimental analysis based on Literature 31

2.9 Terminology 33

CHAPTER 3 METHODOLOGY 35

3.1 Concise methodology 35

3.2 Materials 36

3.3 Production of Micro Crystalline Cellulose (MCC) 36

3.4 Fabrication of Regenerated Cellulose Films 36

3.5 Synthesis of bismuth ferrite nano powder 39

3.6 Preparation of $BiFeO_3$ impregnated RC films 39

3.7 Characterization 40

3.7.1 X-ray Diffraction (XRD) 40

3.7.2 Fourier-transform Infrared (FTIR) Spectroscopy Analysis 41

3.7.3 X-ray Photoelectron Spectroscopy (XPS) 41

3.7.4 Tensile Test 42

3.7.5 Scanning Electron Microscopy (SEM) 43

3.7.6 Light Opacity Test 43

3.7.7 Water Vapor Permeability Test 44

3.7.8 Thermogravimetric Analysis (TGA) 44

3.7.9 UV Visible Diffuse Reflectance Spectroscopy (UV Vis DRS) 45

3.7.10 Nitrogen adsorption desorption isotherm analysis 45

3.8 Photocatalytic degradation of MO 46

3.9 Chemical kinetics and Thermodynamics 48

3.10 Reusability test 51

3.11 Analytic Hierarchy Process 52

CHAPTER 4 RESULTS AND DISCUSSION 55

4.1 Prelude 55

4.2 Determination of the optimum MCC content for photocatalytic films 56

4.2.1 Isolation of Regenerated Cellulose (RC) Films 56

4.2.2 Cellulose dissolution and obtaining regenerated cellulose 58

4.2.3 Degree of Crystallinity of RC Films 60

4.2.4 Chemical interaction between MCC and ionic liquid during Dissolution 62

4.2.5 Tensile Properties of RC Films 65

4.2.6 Morphology of RC Films 67

4.2.7 Light Opacity of RC Films 69

4.2.8 Water Vapor Permeability of RC Films 69

4.2.9 Thermal Degradation of RC films 70

4.2.10 Determination of Optimum MCC Content 73

4.3 Determination of operating conditions for maximum degradation of MO 78

4.3.1 Particle size and size distribution of $BiFeO_3$ particles 78

4.3.2 Chemical nature of $BiFeO_3$ powder and prepared films 80

4.3.3 Surface chemical composition of the photocatalytic films 82

4.3.4 Total chemical composition of the photocatalytic films 83

4.3.5 Crystallinity of the photocatalytic films 85

4.3.6 Forbidden gap of the photocatalytic films 87

4.3.7 BET surface area of the photocatalytic films 90

4.3.8 Morphology of the films 94

4.4 Photocatalytic degradation of MO 96

4.4.1 Degradation experiments 96

4.4.2 Degradation mechanism of MO 101

4.5 Mathematical modelling of MO degradation process 104

4.5.1 Chemical Kinetics 104

4.5.2 Adsorption isotherms 107

4.5.3 Thermodynamic behavior of the system 111

4.5.3(a) The effect of temperature on MO degradation kinetics 111

4.5.3(b) Thermodynamics of adsorption 112

4.6 Reusability study 114

4.6.1 Characterization of photocatalyst using VSM 114

4.6.2 Cyclic experiment 116

CHAPTER 5 CONCLUSION AND FUTURE RECOMMENDATIONS 118

5.1 Conclusion 118

5.2 Recommendations for Future Research 119

REFERENCES 121

APPENDICES

LIST OF PUBLICATIONS

LIST OF TABLES

Page

Table 2.1 Overview of past researches on photocatalysts.....7

Table 2.2 Different cellulose dissolution methods.....16

Table 2.3 Comparison among experimental methods employed by different researches on photocatalytic performance evaluation.....32

Table 2.4 Important terminology 33

Table 3.1 Preparation of buffer solutions with different pH values.....47

Table 3.2 The selected different kinetic models to study the photocatalytic degradation of MO 49

Table 3.3 The selected different adsorption isotherm models to study the adsorption of MO onto photocatalyst.....50

Table 4.1 Crystallinity Indices of RC films and MCC.....61

Table 4.2 Calculation of Available Ionic Liquid Content for MCC Dissolution 62

Table 4.3 Motions of Organic Bonds at FTIR Peak Wavenumbers.....64

Table 4.4 Thermal Degradation Temperatures and Residual Weights of RC films 71

Table 4.5 Rankings Based on Different Application Requirements 74

Table 4.6 Pairwise Comparison and Eigenvector of the RC Films for Photocatalytic applications.....75

Table 4.7 Matrix Obtained by the Pairwise Comparison Made among Alternatives for Every Criterion for Photocatalytic Applications.....75

Table 4.8 Steps for finding the first eigen vector (e_1) for the relative importance of each criterion.....76

Table 4.9 Steps for finding the second eigen vector (e_2) for the relative importance of each criterion.....77

Table 4.10 Steps for obtaining the column vector for tensile properties (CV_{TP}) 77

Table 4.11 Steps for obtaining the column vector for water resistance (CV_{WR}) 77

Table 4.12 Steps for obtaining the column vector for Thermal stability (CV_{TH}) 78

Table 4.13 Steps for obtaining the final eigen vector (e_f) for photocatalytic films 78

Table 4.14 Elemental composition of all RC films.....85

Table 4.15 BET specific surface area, average pore diameter and total pore volume of prepared films and BFO powder.....94

Table 4.16 Parameters obtained for the linear plots of LH, PFO, PSO and IPD models 106

Table 4.17 Calculated parameters of adsorption isotherm models for MO adsorption on RC/BFO film.....109

Table 4.18 Parameters obtained for the linear plots of PSO model for MO degradation at different temperatures.....112

Table 4.19 Thermodynamics adsorption parameters of MO adsorption onto RC/BFO at different temperatures 114

Table 4.20 Magnetization parameters of $BiFeO_3$ powder, pure RC and BFO3.115

Table 4.21 Maximum color removal efficiency variation in cyclic experiment 117

LIST OF FIGURES

Page

Figure 2.1 Oil palm anatomy with important items of the tree 10

Figure 2.2 Demanded cellulose products (a) paper products (b) microcrystalline cellulose..... 11

Figure 2.3 Cellulose polymer chain structure..... 13

Figure 2.4 Intra and intermolecular hydrogen bonded (Supramolecular) structure of cellulose 13

Figure 2.5 Chemical structure of [BMIM]Cl..... 20

Figure 2.6 Cellulose dissolution mechanism inside the ionic liquid [BMIM]Cl 23

Figure 2.7 $BiFeO_3$ Perovskite structure..... 28

Figure 2.8 Schematic diagram on factors affecting on photocatalytic degradation..... 29

Figure 3.1 Concise methodology of the research 35

Figure 3.2 (a) MCC dissolution process inside [BMIM]Cl and (b) solution casting process steps to form thin films 38

Figure 3.3 Photographs of RC films: (a) RC4, (b) RC6.5, and (c) RC9 38

Figure 3.4 Schematic diagram of photocatalytic degradation experiment 48

Figure 3.5 Basic steps of AHP: (a) preparation of criteria eigenvector and (b) finding resultant column vector 54

Figure 4.1 SEM image of MCC using LFD with x10 k magnification 56

Figure 4.2 Particle size distribution of synthesized MCC 56

Figure 4.3 RC films obtained without a stabilizing agent 57

Figure 4.4 RC films obtained from commercial MCC (a) and OPEFB based MCC (b) 58

Figure 4.5 MCC dissolution and coagulation mechanisms to obtain regenerated cellulose film 59

Figure 4.6 FTIR spectrums obtained for commercial [BMIM]Cl (a), TA (b) and the liquid retained after evaporating antisolvent (c) 60

Figure 4.7 XRD patterns obtained for (a) RC4, (b) RC6.5, (c) RC9, and (d) MCC 61

Figure 4.8 FTIR spectra obtained for (a) MCC, (b) RC4, (c) RC6.5, (d) RC9, (e) [BMIM]Cl, and (f) TA 63

Figure 4.9 Stress strain curves of tensile test performed for (a) RC4, (b) RC6.5 and (c) RC9 65

Figure 4.10 Variation of (a) TS and (b) EAB of RC films with respect to MCC content 66

Figure 4.11 (a) Variation of Young's modulus of RC films and (b) comparison of (p) crystallinity index and (q) Young's modulus of RC films with respect to MCC content 66

Figure 4.12 Cross-sectional SEM images of RC films: (a and b) RC4, (c and d) RC6.5, and (e and f) RC9 captured at (a, c, and e) 5000× and (b, d, and f) 10000× magnifications using ETD 68

Figure 4.13 Variation of (a) opacity and (b) water vapor permeability values of RC films with respect to MCC content 70

Figure 4.14 (a) TGA curves and (b) DTG curves of (p) RC4, (q) RC6.5, and (r) RC9 films 72

Figure 4.15 Representation of experimental findings for applying AHP calculations 74

Figure 4.16 Elements of final eigenvalues for RC films used for photocatalytic applications 76

Figure 4.17 SEM image of $BiFeO_3$ using ETD with x 5 k (a) and x100 k (b) magnifications 79

Figure 4.18 Particle size distribution of $BiFeO_3$ powder 79

Figure 4.19 FTIR spectrums obtained for BFO powder (a), MCC, RC and BFO1-5 films (b).....80

Figure 4.20 XPS spectra; C 1s (a), O 1s (b), Bi 4f (c) and elemental mapping Fe 2p of BFO3.....83

Figure 4.21 EDS of pure RC (a) and BFO3 (b).....84

Figure 4.22 XRD patterns of BFO1-5, curves a-e (A) and the comparison of XRD patterns of RC, BFO powder and RC/BFO film (B).....86

Figure 4.23 UV-Vis DRS spectra of RC, BFO and BFO1-3 (a), BFO and BFO3-5 (b), Tauc's plots of BFO (c), RC (d) and BFO1-5 (e-i) and band gap energy variation with BFO content (j).....89

Figure 4.24 N_2 adsorption-desorption isotherms with the corresponding pore size distribution of $BiFeO_3$ powder (a), RC (b) and BFO1-5 (c-g) films 92

Figure 4.25 $P/n(P_o-P)$ vs P/P_o obtained in N_2 adsorption-desorption isotherms for $BiFeO_3$ powder (a), RC (b) and BFO1-5 (c-g).....93

Figure 4.26 SEM images of pure RC (a) and BFO1-5 (b-f) using BSED with x10 k magnification.....95

Figure 4.27 Absorbance values obtained at different wave length values in UV Visible spectroscopy for the all concentrations at pH2 with 3 wt% of $BiFeO_3$ loading 97

Figure 4.28 Color removal efficiency variation at the dark treatment for 10 ppm MO at all pH values with 3 wt% of $BiFeO_3$ loading 97

Figure 4.29 Concentration reduction of MO with time for the all concentrations at pH 2 with 3 wt% of $BiFeO_3$ loading 99

Figure 4.30 Maximum color removal efficiency variation with (a) pH value of 10 ppm MO using 3 wt% of $BiFeO_3$, (b) the concentration of MO at pH 2 using 3 wt% of $BiFeO_3$ and (b) the added $BiFeO_3$ content for the degradation of 10 ppm MO at pH2.....100

Figure 4.31 Appearance of 10 ppm MO at the end of each intermediate treatment during photocatalytic degradation experiment conducted at pH2 with 3 wt% of $BiFeO_3$ loading 100

Figure 4.32 FTIR spectrum obtained for MO solutions before and after photocatalytic treatments 102

Figure 4.33 Possible degradation reactions of MO at direct sunlight 102

Figure 4.34 Possible reaction pathway for MO degradation with intermediates 103

Figure 4.35 The linear fitting plots of LH (a), PFO (b), PSO (c) and IPD (d) models as per the degradation of MO at pH2 with 3 wt% $BiFeO_3$ loading in RC 107

Figure 4.36 (a-e) Freundich, Langmuir, Temkin, D-R and Elovich isotherms for MO degradation with 3 wt% of $BiFeO_3$ and pH 2 with 10 ppm, 15 ppm, 20 ppm and 25 ppm MO concentrations at 30^oC 110

Figure 4.37 PSO kinetic model plots for MO degradation at different temperatures 111

Figure 4.38 Plot of ln (K_d) vs 1/T for the adsorption of MO onto RC/BFO film 113

Figure 4.39 Magnetization behaviour of $BiFeO_3$ powder (A), pure RC and BFO3 films (B) 115

Figure 4.40 Concentration reduction behaviour of MO in cyclic experiment..... 116

Figure 4.41 The appearance of the film (3 wt% of $BiFeO_3$) at the end of each run in cyclic experiment 117

LIST OF SYMBOLS

CV_{TH}	Column Vector of Thermal Stability
CV_{TP}	Column Vector of Tensile Properties
CV_{WR}	Column Vector of Water Resistance
e_1	First eigen vector
e_2	Second eigen vector
e_f	Final eigen vector
e-h	Electron-hole
M	Matrix
M^2	Square matrix
M-H	Magnetization vs applied magnetic field
MCC_{OPEFB}	Oil palm empty fruit bunch based microcrystalline cellulose
R^2	Coefficient of determination in statistical analysis

LIST OF ABBREVIATIONS

AFM	Atomic Force Microscopy
AHP	Analytic Hierarchy Process
[AMIM]Cl	1-allyl,3-methylimidazolium chloride
ASTM	American Society for Testing and Materials
ATR	Attenuated Total Reflectance
BET	Brunauer–Emmett–Teller
BFO	Bismuth Ferrite
[BMIM]Cl	1-butyl-3-methylimidazolium chloride
[BPy]Cl	1-butylpyridinium chloride
BSED	Back Scattered Electron Detector
CMC	Carboxymethyl Cellulose
CNC	Cellulose Nanocrystals
CNF	Citrus Nanofibers
DCA	Dicyanamide
DLD	Delay Line Detector
DMAc	N, N-dimethylacetamide
DMI	1,3-dimethyl-2-imidazolidinone
DMSO	Dimethyl Sulfoxide
D-R	Dubinin-Radushkevich
DRS	Diffuse Reflectance Spectroscopy
DTG	Derivative Thermogravimetry
EAB	Elongation At Break
EBT	Eriochrome Black-T
EDS	Energy Dispersive Spectroscopy
EIS	Electrochemical Impedance Spectroscopy
ETD	Everhart-Thornley Detectors
FAT	Fixed Analyzer Transmission
FTIR	Fourier Transform Infrared
GO	Graphene Oxide
HPLC	High Performance Liquid Chromatography
IPD	Intraparticle Diffusion

LDPE	Low-Density Polyethylene
LFD	Large Field Detector
LH	Langmuir Hinshelwood
MB	Methylene Blue
MCC	Micro Crystalline Cellulose
MFM	Magnetic Force Microscopy
MMT	Montmorillonite
MO	Methyl Orange
NMMO	N-methyl morpholine-N-oxide
NMP	N-methyl-2-pyrrolidine
OPEFB	Oil Palm Empty Fruit Bunch
OPT	Oil Palm Trunk
PF	Paraformaldehyde
PFO	Pseudo First Order
PL	Photo Luminance
PoPD	Poly(o-phenylenediamine)
RC	Regenerated Cellulose
RhB	Rhodamine B
RT	Row Total
SA	Surface Area
SEM	Scanning Electron Microscopy
STP	Standard Temperature and Pressure
TA	Tannic acid
TBAF	Tetrabutylammonium Fluoride Trihydrate
TE	Textile Effluent
TEM	Transmission Electron Microscopy
TGA	Thermogravimetric Analysis
TH	Thermal
TOC	Total Organic Carbon
TP	Tensile Properties
TS	Tensile Strength
UV-Vis	Ultra Violet Visible light
VSM	Vibrational Sample Magnetometry
WR	Water Resistance

WVP	Water Vapor Permeability
WVTR	Water Vapor Transmission Rate
XPS	X-ray Photoelectron Spectroscopy
XRD	X-ray Diffraction

LIST OF APPENDICES

Appendix A Forbidden gap of semiconductors

Appendix B Preparation of RC/BFO nanocomposite films

Appendix C Oral Conference Presentation

PENCIRIAN FILEM SELULOSA DIPERBAHARUI DARIPADA TANDAN BUAH KOSONG KELAPA SAWIT DIGABUNGKAN BERSAMA $BiFeO_3$ BERPOTENSI SEBAGAI FOTOMANGKIN

ABSTRAK

Kecenderungan dalam penggunaan filem selulosa diperbaharui (RC) untuk aplikasi termaju dengan menggunakan polimer semulajadi dan bahan yang dapat diperbaharui telah menunjukkan peningkatan. Degradasi fotomagkin adalah pendekatan novel mersa alam sekitar bagi proses penulenan sisa air. Pada mulanya, filem RC diasingkan melalui teknik penuangan beracuan menggunakan selulosa mikro berhablur berasaskan tandan kosong buah kelapa sawit dan cecair ionik 1-butil-3-metilimidazolium klorida ([BMIM] Cl). Kesan MCC terhadap struktur dan sifat fizikokimia filem RC ditentukan untuk 4% berat, 6.5% berat, dan 9% berat PKS pada suhu 80 ° C. Beberapa kaedah analisis digunakan untuk menilai darjah penghabluran, kestabilan kimia, sifat tegangan , morfologi, kelegapan, kebolehtelapan wap air, dan kestabilan terma filem RC. Keputusan menunjukkan bahawa penambahan 6.5% berat MCC menghasilkan kekuatan tegangan terbaik, 10 MPa. Berbanding dengan filem RC dengan 6.5% berat MCC, kestabilan terma dan kebolehtelapan wap air sedikit meningkat apabila kandungan MCC 9% berat digunakan. Bedasarkan kepada proses hierarki analitik (AHP), 6.5% berat MCC adalah kepekatan MCC terbaik untuk dicampurkan dengan [BMIM] Cl bagi penghasilkan filem RC untuk aplikasi fotomangkin. Pada fasa kedua kajian, (1-5)% berat $BiFeO_3$ sebagai pemangkin ditambah bersandarkan kepada berat MCC ke dalam larutan [BMIM] Cl bagi penghasilan filem nanokomposit RC/BFO. Novel fotomangkin telah disintesis sebagai filem dengan tujuan meningkatkan aktiviti fotokatalitik, kebolehgunaan semula dan kestabilan. Pencirian fotomangkin filem ini dilakukan dengan menggunakan

spektroskopi pantulan sinar UV (DRS), pembalauan sinar-X (XRD), luas permukaan Brunauer-Emmett-Teller (BET), spektroskopi infra-merah transformasi Fourier (FTIR), spektroskopi fotoelektron sinar-X (XPS) dan mikroskopi elektron pengimbasan (SEM). Prestasi fotomangkin filem dinilai dengan merawat pewarna metil oren (MO) di bawah sinar langsung cahaya matahari sehingga penyingkiran warna pewarna yang signifikan dapat diperhatikan. Kepekatan pewarna pada setiap selang waktu ditentukan dengan bantuan spektroskopi UV. Keupayaan pemisahan pemangkin dinilai menggunakan magnetometri sampel Vibrasi (VSM) bertujuan untuk menentukan kebolehgunaan semula. Menurut penemuan dalam pencirian fotokatalitik, $BiFeO_3$ menunjukkan keserasian yang baik dengan RC dan impregnasi $BiFeO_3$ dalam RC tidak mengubah sifat fizikokimia RC secara signifikan. Fotomangkin menunjukkan 90% penurunan pada 10 ppm MO dengan 3% berat $BiFeO_3$ pada pH 2 adalah maksimum dan prestasi pemangkin adalah stabil selama 4 kali kitaran. Corak pengurangan kepekatan MO adalah mengikuti model kinetik urutan kedua pseudo dan penjerapan MO keatas fotokatalis yang disediakan adalah fisisorpsi. Filem nanokomposit RC/BFO ini dijangka boleh digunakan dalam sistem penulenan air yang tercemar daripada sisa pewarna anionik.

CHARACTERIZATION OF REGENERATED CELLULOSE FILMS FROM OIL PALM EMPTY FRUIT BUNCH INCORPORATED WITH $BiFeO_3$ AS A POTENTIAL PHOTOCATALYST

ABSTRACT

There is an increasing interest in regenerated cellulose (RC) films for advanced applications using natural polymers and renewable materials. Also, photocatalytic degradation is an ecofriendly novel approach to purify waste water. Initially, RC films were isolated via solution casting process using oil palm empty fruit bunch (OPEFB) based microcrystalline cellulose (MCC) and the ionic liquid 1-butyl-3-methylimidazolium chloride ([BMIM]Cl). Effects of MCC on the structures and physicochemical properties of the isolated RC films were determined for 4 wt%, 6.5 wt%, and 9 wt% of MCC at 80 °C. Several analytical methods were employed to evaluate degree of crystallinity, chemical stability, mechanical properties, morphology, opacity, water vapor permeability and thermal stability of the RC films. The results showed that the addition of 6.5 wt% of MCC yielded the greatest tensile strength, 10.2 MPA. Compared with the RC films with 6.5 wt% of MCC, thermal stability and water vapor permeability were slightly increased when the MCC content was 9 wt%. According to analytic hierarchy process (AHP), 6.5 wt% of MCC was the best MCC concentration to mix with [BMIM]Cl to manufacture RC films for photocatalytic applications. In the second phase of the study, (1-5) wt% of $BiFeO_3$ with respect to MCC weight was added into the MCC dissolution [BMIM]Cl system for making RC/BFO nanocomposite film as a photocatalyst. The novel photocatalyst was synthesized as a film with the purpose of enhancing the photocatalytic activity, reusability and stability. The photocatalytic characterization of the film was

accomplished by UV visible diffuse reflectance spectroscopy (DRS), X-ray diffraction (XRD), Brunauer–Emmett–Teller (BET) surface area, Fourier transform infrared (FTIR) spectroscopy, X-ray photoelectron spectroscopy (XPS) and scanning electron microscopy (SEM). The photocatalytic performance of the film was evaluated by treating the film with methyl orange (MO) dye under direct sunlight until observe a significant color removal of the dye. The concentration of the dye at each time interval was determined with the aid of UV visible spectroscopy. The catalyst separation capability was evaluated using Vibrational sample magnetometry (VSM) with the purpose of establishing the reusability. According to the findings in the photocatalytic characterization, $BiFeO_3$ shows a good compatibility with RC and impregnation of $BiFeO_3$ in RC does not alter the physicochemical properties of pure RC significantly. The photocatalyst shows 90% degradation of 10 ppm MO as maximum with 3 wt% of $BiFeO_3$ loading at pH 2 and the catalytic performance was stabled for 4 cycles. The concentration reduction pattern of MO follows pseudo-second order kinetic model and the adsorption of MO onto prepared photocatalyst is physisorption. This RC/BFO nanocomposite film was expected to utilize in future water purification systems which are contaminated by anionic dye waste.

CHAPTER 1

INTRODUCTION

1.1 General Introduction

Finding substitutions for petroleum-based non-biodegradable polymers is a demanded field today since the decreasing of non-renewable resources like fossil fuels (Mahmoudian et al., 2012; Zailuddin & Husseinsyah, 2016) and negative environmental impacts affected by synthetic plastics as a result of the accumulation of solid wastes (Mubarak, 2018). Therefore, natural polymers are highly demanded because of their ability to decompose at the end of the life cycle (Keshk & Al-sehemi, 2013). Biopolymers can be synthesized using renewable feedstock derived from plant sources. Those can be yielded by chemical synthesis, starting from basic biological systems. One major category of biopolymers is polysaccharides (Soheilmoghaddam, Sharifzadeh, et al., 2014) and cellulose was identified as the most abundant (Haafiz et al., 2013; Wu et al., 2009; Xia et al., 2016; Zhong et al., 2017) natural polymer (Xiaomin Zhang et al., 2012), largest organic carbon reservoir (Sen Wang et al., 2016a) as well as polysaccharide (Soheilmoghaddam, Sharifzadeh, et al., 2014) on the earth (Zhong et al., 2017).

Industrial wastewater is a highly prevailing environmental concern at present. Wastewater consists of numerous harmful substances to live species. Organic dyes are one of those significant elements which are toxins and carcinogens (Kumar, 2017; Lu Liu et al., 2015). These organic pollutants are used in industries such as textile, plastics, paper, leather and ceramics (Shinde et al., 2017). The presence of these dyes even at very low concentrations may severely effect on ecological systems (Lu Liu et al., 2015). Some examples of unfavorable effects are skin disorders, cancers and gene mutations (Kumar, 2017; Lu Liu et al., 2015). Organic dyes can be identified as cationic and

anionic based on their ionic charge of organic portion. Methylene Blue (MB) is a cationic dye used for silk, paper, wood and leather products while Methyl Orange (MO) is an anionic dye used in textile, printing, scientific research, food and pharmaceutical industries (Lu Liu et al., 2015). Neutralization of these contaminants is a mandatory requirement of industries prior to discharge. Available waste water treatment methods can be classified as physical, chemical and biological operations (Lu Liu et al., 2015). The disadvantage of these conventional methods is the derivation of a secondary sludge which is another burden to biosystems (Kumar, 2017). Photocatalytic degradation of effluent streams is a novel approach as well as an ideal solution to the mentioned subsequent issue.

1.2 Background

Photocatalyst is a substance which utilizes solar energy and perform redox reactions to degrade the organic matter as a result of exciting valence electrons and jumping into conduction band (Kumar, 2017). The energy difference between the bottom of the conduction band and the top of the valence band of a material is known as band gap or forbidden gap. Semiconductors were identified as potential materials to use as photocatalysts due to their less forbidden gap which is the foremost requirement for effective photocatalytic degradation (Du et al., 2018; Gan et al., 2018). Typical semiconductors are TiO_2, ZnS, CdS, ZnO, Cu_2O, BiOX etc and in past years, Bi based compounds were considered as favourable materials for green environmental operations under visible light (Zargazi & Entezari, 2019). Bismuth Ferrite ($BiFeO_3$; BFO) has a perovskite structure which is a magnetoelectric material at room temperature and a visible light photocatalyst for water splitting with a direct forbidden gap of 2.2-2.7 eV. $BiFeO_3$ nanoparticles are superlative for MO degradation (Hongyan Liu et al., 2012).

Therefore, $BiFeO_3$ was selected as the main photocatalytic compound in this research. However, laboratory synthesized $BiFeO_3$ nano powder has several disadvantages such as waste due to difficulty of recollection and agglomeration. Further immobilization of functional materials is the next interesting task with the purpose of enhancing the photocatalytic activity of powdered materials (Zargazi & Entezari, 2019) by introducing a firm geometry. Biopolymers are considered as promising materials in immobilization due to their merits such as biocompatibility, biodegradability, high catalytic activity, high adsorption, low cost, and reusing capability (Du et al., 2018). Scientists have identified that cellulose is a natural polysaccharide which can be decomposed at the end of its life cycle. This valuable biopolymer is the basic structural component of plants. It can be isolated from numerous sources and Palm oil tree is one of those sources. According to Haafiz et al. in 2013, microcrystalline cellulose (MCC) was isolated from oil palm empty fruit bunch (OPEFB) (Mohamad Haafiz et al., 2013). This powder form MCC can be dissolved in a desired solvent to obtain different geometries such as hydrogels, films and fibers (Sen Wang et al., 2016b). Such an output is known as regenerated products which are used in applications such as packaging, biomedical, optical, electronic, water treatment and membranes (Soheilmoghaddam, Wahit, et al., 2014). Therefore, in this research, regenerated cellulose (RC) was selected as the immobilizer for powder form $BiFeO_3$.

1.3 Problem Statement

As explained in section 1.1, conventional water treatment methods generate subsequent waste which should be additionally treated. Therefore, eco-friendly waste water neutralization techniques are highly demanded. On the other hand, depletion of petroleum resources as non-renewable resources and accumulation of synthetic polymer

waste are enormous problems for next generation. Therefore, renewable bio-based materials are extremely necessitated to substitute the synthetic polymer requirements. Further, laboratory synthesized $BiFeO_3$ nano powder has several disadvantages such as post operational waste of used powder due to difficulty of recollection and agglomeration. Therefore, immobilization of functional materials is the next interesting task with the purpose of enhancing the photocatalytic activity of powdered materials (Zaahari et al., 2019) by introducing a stable geometry.

1.4 Scope of the study

In this research, degradation of MO was evaluated with the aid of $BiFeO_3$ impregnated RC nanocomposite films as a photocatalyst. MCC was used as the cellulose source to obtain RC films by dissolving MCC in ionic liquid 1-butyl,3-methylimidazolium chloride [BMIM]Cl and solution casting method. Initially the required best amount of MCC weight was determined by synthesizing pure RC films and subsequent characterization. Chemical stability, thermal stability, light opacity, water vapour permeability (WVP) and tensile properties of pure RC films were evaluated with the aid of Fourier transform infrared spectroscopy (FTIR), thermogravimetric analysis (TGA), light opacity analysis, WVP analysis and tensile test respectively. Analytic hierarchy process (AHP) was employed on the observed characterization results to define the best MCC content for incorporating with $BiFeO_3$ to produce photocatalytic films.

That MCC content was included with (0-5) wt% of $BiFeO_3$ with respect to MCC weight inside the MCC dissolution ionic liquid system. Chemical nature of the prepared photocatalysts were examined by FTIR and X-ray photoelectron spectroscopy (XPS) analysis. Light absorption capability of those films was evaluated by UV visible diffuse

reflectance spectroscopy (DRS). The efficiency of catalytic performance was measured by N_2 adsorption desorption isotherm Brunauer Emmett Teller (BET) surface area analysis. The crystalline nature of photocatalysts was analyzed with the aid of X-ray diffraction (XRD). Morphology of raw materials and products were observed using scanning electron microscopy (SEM). Also, energy dispersive X-ray spectroscopy (EDS) was employed on the prepared RC/BFO films to determine the effectiveness of impregnation of $BiFeO_3$ inside the RC matrix. The photocatalytic performance of the film was evaluated by treating the catalyst dye mixture under direct sunlight until observe a significant color removal of the dye. The irradiation experiments were conducted for different concentrations (10 ppm, 15 ppm, 20 ppm and 25 ppm) with different pH (2, 4, 6, 8 and 10) values of MO dye. The concentration of the dye at each time interval was determined with the aid of UV visible spectroscopy.

The identified best process conditions were applied for reaction kinetic study of the degradation process using 4 different models such as Langmuir Hinselwood, Pseudo first order, Pseudo second order and Intraparticle diffusion models. Adsorption isotherms were studied using 5 different models such as Freundich, Langmuir, Temkin, Dubinin-Radushkevich (D–R) and Elovich isotherms. Thermodynamics of MO adsorption onto RC/BFO film was studied by conducting the photocatalytic degradation at 5 different temperatures (30^{o}C, 40^{o}C, 50^{o}C, 60^{o}C and 70^{o}C) using the maximum degradation conditions.

1.5 Gap of novelty

Minxing Du.et al in 2018 have developed a photocatalyst using BiOBr with RC for Rhodamine B (RhB) (cationic dye) degradation under visible light (Du et al., 2018). Mahboobeh Zargazi and Mohammad H. Entezari in 2019 have prepared a $BiFeO_3$

coated stainless steel mesh as a photocatalyst for phenol degradation under visible light (Zargazi & Entezari, 2019). Also $BiFeO_3$ based $(Na_{0.5}Bi_{0.5})TiO_3$ butterfly wings have been prepared by Hongyan Liu et al in 2012 for RhB degradation under visible light (Hongyan Liu et al., 2012). Further Atilia et al in 2019 have synthesized a hydrogel consists of carboxymethyl cellulose (CMC) and $BiFeO_3$ for the degradation of MO (Zaahari et al., 2019). However, the selected approach is a nanocomposite film made of RC and nano $BiFeO_3$ by solution casting which has not been studied previously. This research was aimed to synthesize the photocatalyst as a film since it is the most appropriate and convenient geometry to immobilize the powder photocatalyst using RC. In addition to that, it is expected to gain the opportunity of reusing the photocatalyst for several times with the film geometry.

1.6 Objectives

Research objectives can be described as follows.

1) To characterize the regenerated cellulose (RC) obtaining from oil palm empty fruit bunch based microcrystalline cellulose (MCC_{OPEFB}) using different MCC content.
2) To determine the optimum operating conditions such as $BiFeO_3$ composition in RC matrix, pH and concentration of MO for the maximum degradation of methyl orange (MO)
3) To propose the most appropriate kinetic model for the observed maximum photocatalytic degradation of MO
4) To define the adsorption mechanism of MO onto the photocatalyst surface with the aid of isotherm modeling and thermodynamics study

CHAPTER 2

LITERATURE REVIEW

2.1 General Overview

Previous research efforts have been made with different photocatalyst materials and geometries as summarized in Table 2.1. In column 2 of Table 2.1, catalyst loading is the weight of active catalyst (g) immersed in the selected organic dye volume (l) (Du et al., 2018; Gan et al., 2018; He et al., 2019; Hongyan Liu et al., 2012; Sivakumar et al., 2019; Zargazi & Entezari, 2019). This chapter explains the development of cellulose dissolution processes since preliminary efforts, the process of photocatalytic water purification and the selection of experimental methods to characterize the photocatalyst.

Table 2.1 Overview of past researches on photocatalysts

Geometry of Photocatalyst	Catalyst loading (g/l)	C_o (ppm)	Organic dye	Light Source
BiOBr/cellulose gel	0.4	25	RhB (Rhodamine B)	500W high pressure Xe lamp equipped with UV cut-off filter to provide visible light ($\lambda \geq 420$ nm)
$BiFeO_3$ Thin coating on stainless steel mesh	Not mentioned	Not mentioned	Phenol	Xe lamp with cut-off filter ($\lambda \geq 400$ nm)

Bi/La VO_4/PoPD Nano rod	0.5	15.75	MB/TE (Textile Effluent)	Two 250W Xe lamps with $\lambda \geq 420$ nm
$BiFeO_3$–$(Na_{0.5}Bi_{0.5})TiO_3$ Replica	2	5	RhB	350W Xe lamp
Cellulose based carbon microspheres incorporated by $CoFe_2O_4$ Composite	0.25	20	RhB	500W tungsten lamp
$CoFe_2O_4$.PoPD hetero junction	0.5	20	Tetracycline	300W Xe lamp, 1.8x105lx

2.1 Biopolymers

Plants produce more than ten billions of tons of cellulose per annum globally (Sen Wang et al., 2016a). Cellulose is a harmless substance to the environment since it can be decomposed and connected with the natural carbon cycle after a simple decay reaction (Suhas et al., 2016). Cellulose has a predictable annual production of $90x10^9$ metric tons and denotes the most noticeable renewable (Kosan et al., 2010) resource for manufacturing bio composites (Pinkert et al., 2009). This natural polymer exhibits outstanding properties (Fink et al., 2001), which is utilized in applications such as paper, textile, artificial fibers, membranes (Mahmoudian et al., 2012), water treatment (Mahmoudian et al., 2012; Sen Wang et al., 2016a), biofuel (Reddy et al., 2017), biomedical applications (Soheilmoghaddam, Wahit, et al., 2014), optical and electrical

devices (Sen Wang et al., 2016a). Cellulose was discovered in 1838 by the scientist Anselme Payen (Isik et al., 2014) by isolating it from a plant material with the purpose of deriving its chemical formula (Hina et al., 2015). Later on, the first improved cellulose was revealed by Braconnot in 1839 (Suhas et al., 2016).

In Malaysia and Indonesia, biomass resources are mostly generated by the palm oil industry (Abdulrazik et al., 2017; Chang, 2014; Theo et al., 2017). In Southeast Asia and South America, oil palm is the major source of vegetable oil (De Farias et al., 2018). Oil palm tree has been identified as a potential cellulose source since its trunk to disposals are raw materials for the significant cellulose allied product outputs. Figure 2.1 shows a sketch of an oil palm tree with its anatomy while Figure 2.2 displays some demanded cellulose product outputs . In Malaysia, there is a significant amount of biomass including palm kernel shells (PKS), oil palm trunk (OPT), oil palm empty fruit bunch (OPEFB) and mesocarp fruit fiber. The OPEFB is a solid waste retained after palm oil milling process and its annual accumulation rate is 1.24 million tons. Therefore, OPEFB is a readily available biopolymer to utilize in value added applications (Nor Amalini et al., 2019a).

Naturally, cellulose is not meltable (Fink et al., 2001) and less water soluble. Less water solubility is the main challenge for cellulose bioprocessing since it is difficult to dissolve in water and some other solvents (Mohd et al., 2017). The first attempt to dissolve cellulose was made in early 1920 (Pinkert et al., 2009) with the aid of some aqueous and nonaqueous solvents. At the end of 90 decade researchers have endeavored to identify ionic liquids as a potential solution to dissolve cellulose and prepare RC (Turner et al., 2004) because of their attractive properties like negligible vapor pressure (Pinkert et al., 2009), low melting point (Turner et al., 2004; Zhu et al., 2006), chemical and thermal stability and non-flammability (Zhu et al., 2006). In this

description, use of ionic liquids on cellulose dissolution and the unique features of commercially available ionic liquids are discussed as key titles.

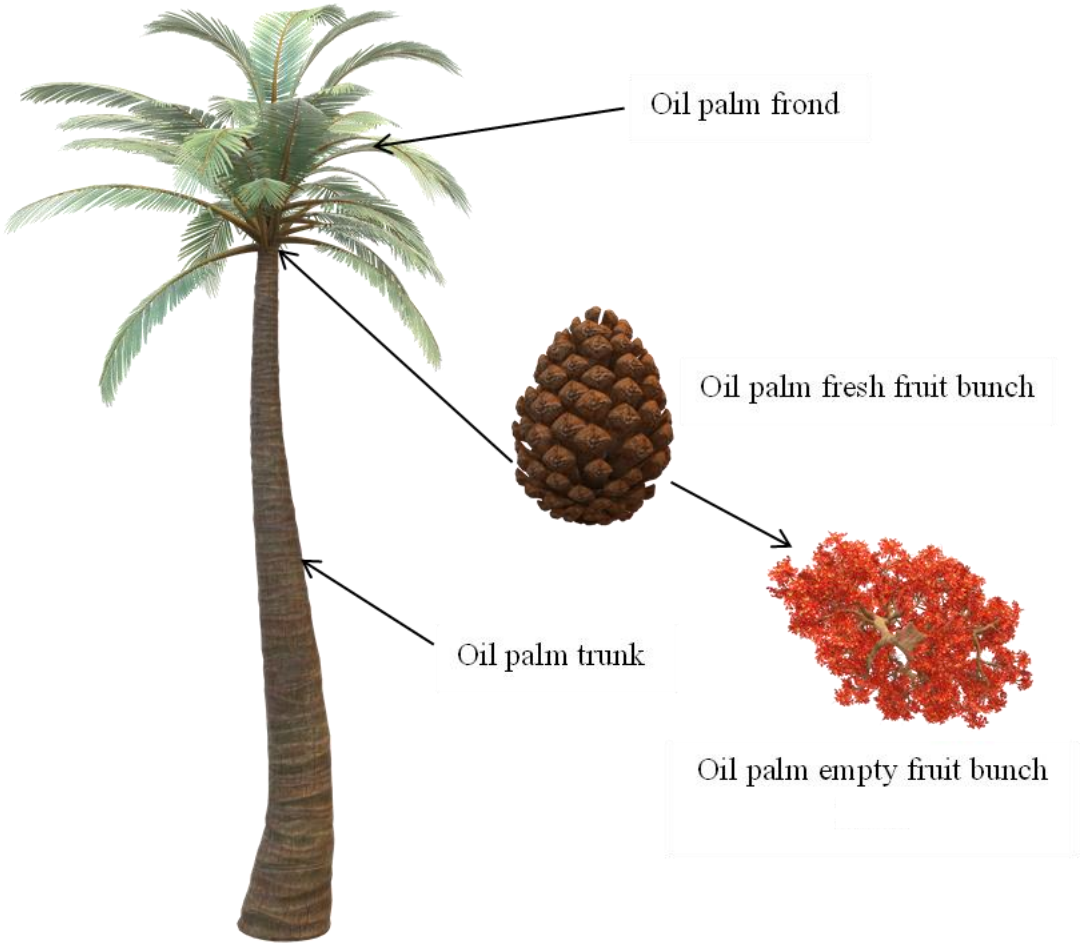

Figure 2.1 Oil palm anatomy with important items of the tree

Figure 2.2 Demanded cellulose products (a) paper products (b) microcrystalline cellulose

2.2 Development of cellulose dissolution processes

2.2.1 Cellulose and its nature

As a whole, biomass consists of cellulose (35-50%), hemicellulose (20-35%) and lignin (10-25%) (Marett et al., 2017; Hua Zhao et al., 2009). Cellulose is a linear carbohydrate (Tong Zhao et al., 2018), a homopolymer of glucose ($C_6H_{10}O_5$) with repeating units comprising of β-D-glucose in $^4C_1$ conformation as shown in Figure 2.3 while lignin and hemicellulose have branched structures (Pinkert et al., 2009). Naturally, microfibril or high crystalline structures are obtained as a result of the interconnection of 40-70 adjacent cellulose chains between C_6 hydroxymethyl and C_3 hydroxy groups by hydrogen bonds. Native cellulose is a semicrystalline polymer (Rosli et al., 2015) with microfibrils and certain amorphous parts (Pinkert et al., 2009) wherein the structure is known as a hydrogen-bonded supramolecular structure (Hua Zhao et al., 2009) as depicted in Figure 2.4. It is insoluble in water as a result of supramolecular structure and can be degraded by microbial fungal enzymes (cellulase) (Mohamad Haafiz et al., 2013). Cellulose is a typical example of a renewable and biodegradable structural plant polymer which can be processed into Whisker-like micro fibril (Fink et al., 2001). It is one of the most significant and attractive natural resources because of

biodegradability, low density and excellent mechanical properties such as great stiffness and strength (Collazo-Bigliardi et al., 2018). Cellulose crystal regions are a bundle of stretched cellulose chain molecules with a young's modulus of around 137 GPa (Cheng et al., 2007). Intramolecular hydrogen bonds are responsible for the linear integrity and rigidity of the polymer chain while intermolecular hydrogen bonds serve the aggregation of multiple chains to form crystals (Roslan, 2015). The size of the chain depends on the degree of polymerization (Pinkert et al., 2009). Due to higher degree of polymerization, cellulose has fewer chain ends compared to starch which has lesser degree of polymerization (Hua Zhao et al., 2009). The number of glucose units for wood, native cotton and bacterial cellulose are 10000, 15000 and 10000 respectively (Pinkert et al., 2009). As explained by Zhang et al in 2004, cellulose is tangled with hemicellulose and lignin in nature (Hua Zhao et al., 2009). Even though hydrogen bonded cellulose network hinders the dissolution of cellulose, intrinsic -OH groups have an affinity to inorganic and organic substances that aid the preparation of hybrid materials and expand the potential applications of cellulose as functional materials (Sen Wang et al., 2016a). Cellulose hydrolysis is facilitated by mineral acids and cellulases as catalysts to yield glucose as the end product (Emanuelsson, 1996). As explained by Ranby in 1951, It is convenient to hydrolyze the amorphous regions of native cellulose with the aid of a strong acid (Mohamad Haafiz et al., 2013).

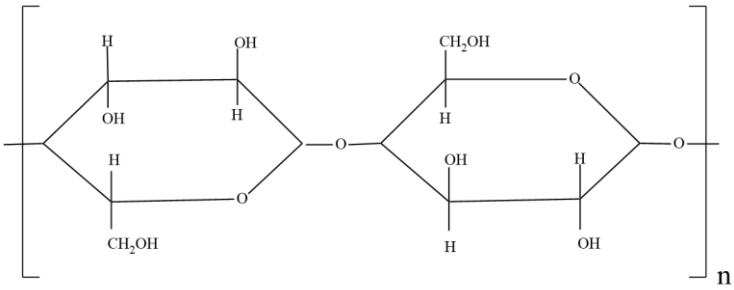

Figure 2.3 Cellulose polymer chain structure

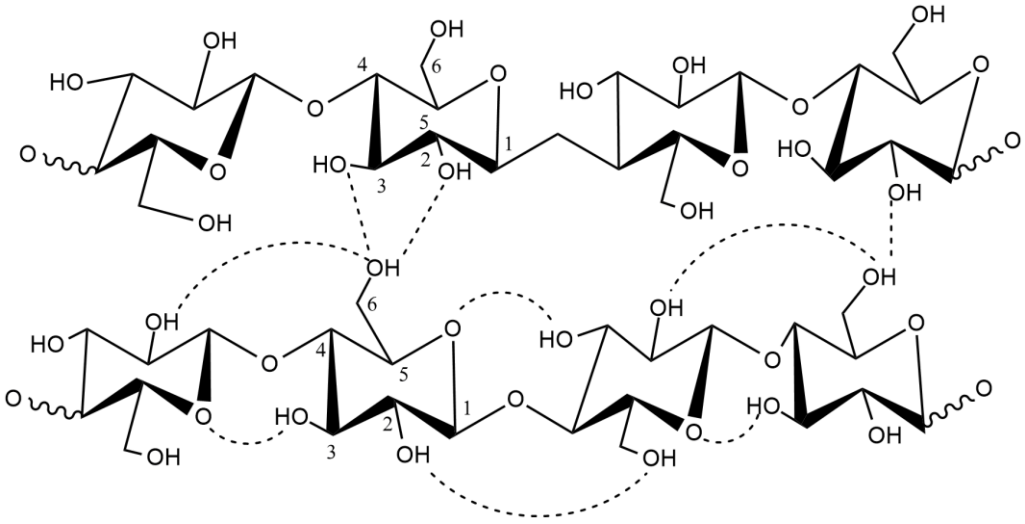

Figure 2.4 Intra and intermolecular hydrogen bonded (Supramolecular) structure of cellulose

2.2.2 Cellulose Dissolution

2.2.2(a) Preliminary research works

Cellulose dissolution is a massive challenge as a result of its crystalline and branched (Reddy et al., 2017) structure donated by microfibrils (Mohd et al., 2017). Figure 2.4 depicts the supramolecular structure of cellulose and as a result of this structure, chemical processing of cellulose is extremely difficult and insoluble in water and most of the organic liquids (Reddy et al., 2017; Yang et al., 2010). An adequate

biomass pretreatment and depolymerization methods are essential to utilize the plant biomass effectively and efficiently (Engel et al., 2010). Most of the available methods are mechanical, chemical, biological and physicochemical pretreatments. Mechanical milling needs high energy but unable to remove lignin while chemical methods are expensive and suitable for high value paper products only. On the other hand, biological or fungal treatments require long residence time about 10-14 days. Physicochemical treatments such as steam explosion demand high temperature, pressure and catalysts (Hua Zhao et al., 2009).

A desirable cellulose solvent should have low toxicity, ease of recycling, low viscosity, high thermal stability and moderate melting temperature. But, all of these properties have not been satisfied together yet (Mohd et al., 2017). Up to date researchers have made attempt to dissolve cellulose by two main methods as viscose and non-viscose. In viscose method, cellulose is converted into sodium cellulose xanthate with the use of CS_2. The obtained cellulose xanthate is soluble in NaOH and therefore the solution can be used to produce fiber or film using wet spinning technique (De Silva et al., 2015). On the other hand in non-viscose process, cellulose is dissolved by employing several solvents such as urea/NaOH, N-methyl morpholine-N-oxide (NMMO), LiCl/N-methyl-2-pyrrolidine (NMP), LiCl/1,3-dimethyl-2-imidazolidinone (DMI), dimethyl sulfoxide (DMSO)/paraformaldehyde (PF)(Hao Zhang et al., 2005), (DMSO)/tetrabutylammonium fluoride trihydrate (TBAF) (Cao et al., 2009; Zhen Liu et al., 2011; Pang et al., 2015), LiCl/N,N-dimethylacetamide (DMAc) (Hao Zhang et al., 2005), some molten salt hydrates like $LiClO_4.3H_2O$ and $LiSCN.2H_2O$ (Cao et al., 2009), $ZnCl_2$ and ionic liquids (ILs) (Zheng et al., 2019). Depending on the association of the solvent molecules with polysaccharide, solvents are classified as derivatizing and non-derivatizing. Derivatizing solvents interact with the cellulose hydroxy groups and

form intermediates. In derivatizing processes cellulose is subjected to a chemical reaction while cellulose undergoes entire physical process with non-derivatizing solvents during dissolution (Sen Wang et al., 2016a)

Even though the first challenge to dissolve cellulose moves back to early 1920 (Pinkert et al., 2009), those methods have not been succeeded due to the high environmental poisonousness and insufficient solvation power (Pinkert et al., 2009). Although, acid hydrolysis activates cellulose dissolution, it leads the formation of undesirable degradation products of glucose as well as corrosion prevention is required in handling process (Emanuelsson, 1996). Table 2.2 includes different methods investigated during past decades by researches on dissolution of cellulose. Microwave heating accelerates cellulose dissolution process significantly and it aids to reduce the dissolution time and energy consumption (Sen Wang et al., 2016a). The processes explained in Table 2.2 are known as traditional processes (Zhu et al., 2006) and those serve several disadvantages as explained here.

Table 2.2 Different cellulose dissolution methods

Method	Additive/Solvent	Advantages	Disadvantages
Milling	This is a mechanical method	A chemical free method	Needs high energy, unable to remove lignin
Chemical viscose	CS_2 , NaOH, H_2SO_4	The obtained cellulose xanthate is soluble in NaOH and therefore the solution can be used to produce fiber or film using wet spinning technique	Causes heavy pollution due to H_2S, SO_2, strong base (NaOH), Required harsh conditions and difficult to maintain so that expensive, limited to laboratory scale
Chemical non viscose	Urea/NaOH, NMMO, LiCl/ NMP, LiCl/DMI, DMSO/ PF, DMSO/ TBAF, LiCl/ DMAc, some molten salt hydrates like $LiClO_4.3H_2O$ and $LiSCN.2H_2O$, $ZnCl_2$ and ionic liquids	Ionic liquids can be recovered after dissolution process	Long incubation time, brings environmental burdens, expensive, obstinate, required high energy to operate
Microwave heating		Reduced energy consumption and dissolution time	Expensive

Biological/Fungal treatments		Environmentally friendly process, less harmful	Long residence time (10-14 days)
Steam explosion		Efficient process	Demand of high temperature, pressure and catalysts, expensive

2.2.2(b) Ionic liquids

All above mentioned dissolution techniques have intrinsic disadvantages like volatility of DMAc/LiCl, recovering difficulty of NaOH/urea, toxicity of DMSO/TBAF, and instability of NMMO in application. Ionic liquid was first discovered in 1914 by Walden (Pinkert et al. 2009) and first organic molten salt system was developed in 1934 as N-ethylpyridimium chloride. But its commercial usage has been avoided since the high melting point at around 120^{o}C. In the 1960s at the U.S Air Force Academy has experimented binary mixtures of 1-butylpyridinium chlorides ([BPy]Cl) and aluminum chlorides ($AlCl_3$) as salt electrolytes for thermal batteries. But these first-generation ionic liquids have had disadvantages such as prompt electrochemical reduction and air sensitivity (Pinkert et al. 2009). These problems could have been overcome at the beginning of 1990s with second-generation ionic liquids which were air and water-stable (Pinkert et al. 2009). The popular examples of these ionic liquids are salts of organic cations (alkylimidazolium $[R_1R_2IM]^+$, alkylpyridinium $[RP_y]^+$, tetraalkylphosphonium $[PR_4]^+$, and tetraalkylammonium $[NR_4]^+$ and anions (nitrate $[NO_3^-]$, tetrafluoroborate $[BF_4^-]$, hexafluorophosphate $[PF_6^-]^-$, trifluoromethane sulfonate (triflate) $[CF_3SO_3^-]$, methane sulfonate (mesylate) $[CH_3SO_3^-]^-$, and bis-(trifluoromethanesulfonyl)amide $[Tf_2N^-]$. Also, anions of low

melting point such as chloride, bromide, and iodide salts were also utilized in several applications (Pinkert et al. 2009).

However, at the end of 90-decade, researchers have recognized ionic liquids with low melting point and low vapor pressure as a potential source in industry and research (Turner et al. 2004a). In this scenario, liquid phase salts around the room temperature which are stable up to temperatures of about 300^{o}C are known as ionic liquids (Pinkert et al., 2009). Those are composed of an organic cation and an inorganic anion (Mohd et al. 2017a). Robin D.Rogers has received US Presidential Green Challenge award in 2005 for verifying that ionic liquids are capable of physically dissolving cellulose (Wang et al. 2016). Nowadays ionic liquids are utilized as solvents for cellulose regeneration and as a reaction media for homogeneous modification of cellulose (Lu et al. 2015).

Ionic liquids are made of salts of organic cations (imidazolium salts) (Pinkert et al. 2009) with short side chains (Quan et al., 2010). Some of the most prevalent commercial ionic liquids are 1-butyl,3-methylimidazolium chloride ; [BMIM]Cl, 1-allyl,3-methylimidazolium chloride ; [AMIM]Cl, 3-methyl-N-butylpyridinium chloride; C_4[mpy]Cl etc (Pinkert et al., 2009). Singh and coworkers have found that the interaction energy between the cellulose chain and the ionic liquid was stronger than that for chain/water or chain/methanol interactions (Wang et al. 2016). Melting temperature and viscosity of the ionic liquid depend on the type of anion (Pinkert et al. 2009).

Ionic liquids are utilized in biological applications (biocatalysts, biosensors etc.), chemical engineering requirements (separation processes, polymer and catalytic chemistry, lubricants, substitution for another solvent, electrolytes) and other advanced technological devices (optical thermometers, lunar telescopes etc.) (Pinkert et al. 2009)

2.2.2(c) [BMIM]Cl

Heinze et al. (2005) has measured ^{13}C nuclear magnetic resonance spectra for a finished product after dissolution of raw cellulose in [BMIM]Cl and they have confirmed that [BMIM]Cl is a non-derivatizing solvent (Zhao et al. 2009). Swatlokksi et al. in 2002 has discussed the use of an ionic liquid as solvent for the regeneration of cellulose and for the chemical modification of the polysaccharide (Pinkert et al. 2009). Further they have identified that [BMIM]Cl has a good dissolving power (Mahmoudian et al. 2012) without derivatization in high concentrations of cellulose (Zhang et al. 2005). In 2005, Moulthrop et al. has synthesized regenerated cellulose using [BMIM]Cl as the ionic liquid. The structure of RC film was examined using X-ray powder diffraction and it proves the reduced crystallinity of film. Further, they have proved the improved enzymatic hydrolysis kinetics of [BMIM]Cl (Emanuelsson 1996). Numerous types of materials such as membranes, beads and hollow fibers can be yielded by cellulose processing at room temperature using [C_4mim]Cl or [BMIM]Cl (Turner et al. 2004a). In addition to that it is a hydrophilic ionic liquid (Soheilmoghaddam et al. 2014b) as well as completely miscible with water in any ratio (Liu et al. 2011). Methylimidazolium and methylpyridinium allied with allyl-1, ethyl-1 or butyl-1 side chains are ideal cations for cellulose dissolution. Even numbers of carbon atoms in the side chain show high cellulose dissolution in the series of C_2 to C_{20} compared with odd numbers. The maximum dissolution power is accomplished with the C_4 side chain and the incorporated hydroxy atoms are capable to enhance the solubility of cellulose (Pinkert et al. 2009). This is because of the additional polarity in the heteroatomic substituents on the imidazolium ring. Double bond comprising side chains reduces the viscosity of the ionic liquid. The same effect has been observed when one of the alkyl chain carbon atoms is substituted by an oxygen atom (Pinkert et al. 2009). Cellulose

dissolving ionic liquids comprise anions of chloride (Cl^-), acetate (CH_3COO^-) or formate ($HCOO^-$) because of their ability to form strong hydrogen bonds (Zhao et al. 2009a). Chloride was selected from halogen series (halides) due to high polarity (Amalini et al. 2019). Cellulose can form a hydrogen bond with chloride ions at elevated temperature (Zhao et al. 2009a). Above aetiology interferes to propose [BMIM]Cl as a best ionic liquid for cellulose dissolution and RC manufacturing process. Figure 2.5 depicts the chemical structure of [BMIM]Cl.

Further ideal dissolution temperature is 10^oC above the melting point of ionic liquid (Pinkert et al. 2009). Melting point of [BMIM]Cl is around 70^oC (Zhao et al. 2009a) and therefore it can be recommended to maintain 80^oC as the most suitable operating temperature for cellulose dissolution experiments with [BMIM]Cl.

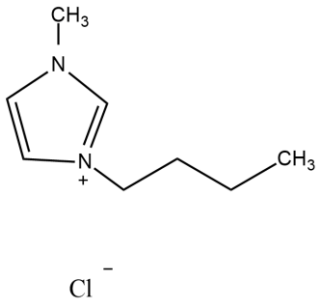

Figure 2.5 Chemical structure of [BMIM]Cl

2.2.2(d) Advantages of ionic liquids

Compared with homogeneous cellulose derivatization in other solvents, the main advantages of room temperature ionic liquids are simple separation of products and solvents, thermal stability, short process time, potential electrochemical applications, catalyst free process, absence of by-products etc. (Cao et al., 2009). Further these ionic liquids comprise low vapor pressure and high solvation ability towards various chemical substances. As a result of low vapor pressure of ionic liquids, solvent evaporation is minimized and the precautions on respiratory protection and

exhaust systems can be limited (Pinkert et al. 2009). Therefore recyclability of ionic liquids (Pinkert et al. 2009) is enhanced and ionic liquids can be utilized in a wide range of applications (Cao et al., 2009; Yao Li et al., 2018). Ionic liquids can be defined as molten salts with melting temperature less than 100 °C, and having the ability to dissolve lignin (Pinkert et al. 2009). In the environmental point of view and concerning the economy, ionic liquid recovery after usage is an interesting topic. In RC manufacturing process, ionic liquid is dissolved inside a coagulation water bath. One simple operation is separating ionic liquid by evaporating water at 100^{o}C and reduced pressure since the ionic liquids are stable up to 300^{o}C. In the case of [AMIM]Cl, it has been recovered and the confirmation has been made by ^{1}H NMR spectroscopy. According to the analysis, recovered ionic liquid had purity of 99% and reusing capability. However, membrane technologies such as nanofiltration, reverse osmosis and pervaporation and salting out of ionic liquid in large scale industrial process are several suggestions for ionic liquid recovery in future (Cao et al., 2009).

2.2.2(e) Dissolution process of cellulose

Detailed cellulose dissolution mechanism is still under investigation. In general, it is known that the dissolution interferes the complex structure of cellulose while conserving chemistry (Engel et al. 2010). Ideally all hydrogen bonds within the cellulose microfibrils are broken during the dissolution process (Pinkert et al. 2009). In the actual dissolution process, cation is attracted to the end of oxygen atom which is connected with polar hydrogen atom and anion is attracted to that released polar hydrogen atom. Figure 2.6 demonstrates the mechanism concisely if the used ionic liquid is [BMIM]Cl. The efficient dissolution of cellulose is an challengeable task in cellulose research and development (Pinkert et al. 2009).

Cellulose dissolution is spontaneous and exothermic process wherein hydrogen bonding accepting ability (β value) of the anions is the determinant of the solubility of cellulose in a specific media. The β value obtained in the solvatochromatic study was a good indicator of the ability to dissolve cellulose. Chemical structure of imidazolium cations plays a key role with cellulose dissolution. Anions such as $[BF_4]^-$, $[PF_6]^-$, $[Tf_2N]^-$ are not effective solvents as a result of the weak hydrogen bond basicity. When the chain length of alkyl groups increases, symmetry of cations tends to increase. The dissolution rate of cellulose in ionic liquid is reduced due to the increase of viscosity and decrease of hydrogen bond acidity (Li et al. 2018). Dissolving ability of the following cations and anions is decreased as follows:

Cations

(Imidazolium based >Pyridinium based >Ammonium based) ionic liquids

Anions

Acetoxy[OAc]->$[HSCH_2COO]^-$>[HCOO]->$[C_6H_5COO]^-$ >$[H_2NCH_2COO]$>$[HOCH_2COO]^-$> >$[CH_3CHOHCOO]^-$>dicyanamide[DCA] (Li et al. 2018)

In dissolution process, the anion interacts with polar region by electrostatic force and cation links with glucon ring by non-polar van der waals forces. Formed hydrogen bonds could not be substituted by internal hydrogen bonds of cellulose when anions are $[OAc]^-$, $[Cl]^-$ and dimethyl phosphate [DMP]. Co solvents such as DMSO and water can mix with ionic liquid with the purpose of cost reduction (Li et al. 2018)

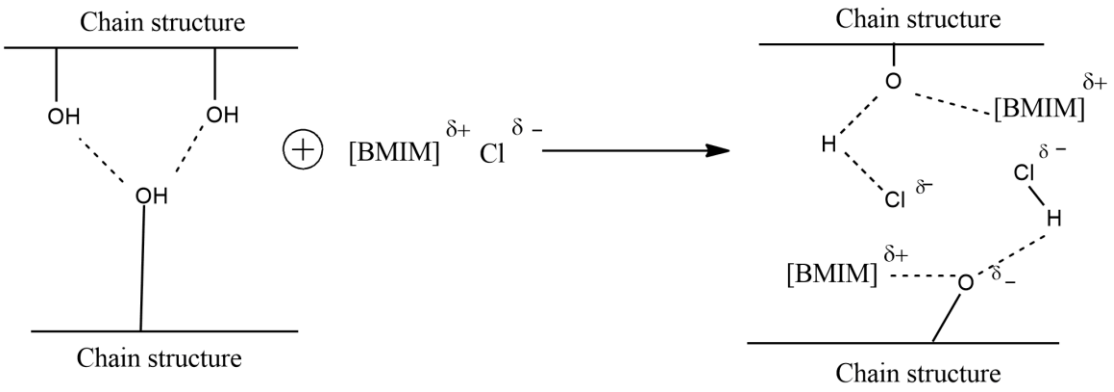

Figure 2.6 Cellulose dissolution mechanism inside the ionic liquid [BMIM]Cl

2.3 Regenerated cellulose

After completion of cellulose dissolution, an antisolvent can be introduced to decrease the solubility of the solute (cellulose) in the used solvent (ionic liquid). As a result, the solute is precipitated, and the solvent is dissolved in the antisolvent (Chemistry et al., 2007). Cellulose separation can be accomplished by this phenomenon and is called "regeneration". Compressed CO_2, ethanol, methanol, deionized and distilled water are some known antisolvents (Dadi et al., 2006).

Typically, RC materials are prepared from cellulose solution through physical dissolution and shaping (Wang et al. 2016). The shape of the regenerated material depends on the regeneration method and conditions. Thin films with a thickness between 0.1 mm and 0.2 mm can be obtained by solution casting (Mahmoudian et al., 2012; Nor Amalini et al., 2019a). Electrospinning is done by injecting the dissolved cellulose melt into a coagulation bath to yield cellulose fibers. Tissue engineering scaffolds are another demanded RC application in modern world. RC/β-cyclodextrin(RC/β-CD) scaffold was prepared by particulate leaching technique with the aid of [BMIM]Cl (Soheilmoghaddam, Sharifzadeh, et al., 2014). Further bio regenerated cellulose/sepiolite nanocomposite films were also prepared using

[BMIM]Cl with the purpose of applying those films in membranes, biomaterials and food packaging units (Soheilmoghaddam, Wahit, et al., 2014). Also RC ultra filtration membranes were modifies using aqueous, surface-initiated atom transfer radical polymerization with the purpose of adjusting the pore size of the membrane in the process of polymerization (Singh et al., 2008). Cornhusk regenerated cellulose films were synthesized using the ionic liquids [Amim]Cl) and 1-ethyl-3-methylimidazolium acetate [Emim]Ac (Yang et al., 2010).

The process parameters ; dissolution time and precipitation rate are affected by the initial cellulose concentration of the solution (Pinkert et al. 2009).

2.4 Microcrystalline cellulose (MCC) and experimental selection for optimizing the process

Cotton liners and wood pulp were identified as the main source for commercial cellulose production. In fact, these raw materials are quite expensive and therefore lignocellulosic biomass were recognized as a potential solution to utilize as cellulose sources (Yang et al., 2010). Natural lignocellulosic biomass is composed of crystalline and amorphous regions of the physical molecular chain structure. Scientist Battista in 1950 has introduced a methodology to obtain microcrystalline cellulose (MCC) starting from native cellulose using 2.5 N HCl at 105 °C for 30 min with constant agitation in the ratio of 1:20 pulp to liquor as a result of hydrolyzing the amorphous regions without weight loss (Mohamad Haafiz et al., 2013). Therefore, the newly obtained material is enriched with crystalline regions and its average particle size exists in micron range (~100 μm) (Ohwoavworhua & Adelakun, 2010). So that MCC is a fine, odorless and biodegradable powder which has unchanged cellulose I type with improved crystallinity (Mohamad Haafiz et al., 2013). In fact, MCC is a partially depolymerized cellulose